J Soils Sediments (2012) 12:1435–1444
DOI 10.1007/s11368-012-0542-9

SEDIMENTS, SEC 2 • PHYSICAL AND BIOGEOCHEMICAL PROCESSES • RESEARCH ARTICLE

Nitrate reduction coupled with microbial oxidation of sulfide in river sediment

Xunan Yang · Shan Huang · Qunhe Wu · Renduo Zhang

Received: 24 December 2011 / Accepted: 19 May 2012 / Published online: 26 June 2012

Abstract
Purpose Nitrate (NO_3^-) is often considered to be removed mainly through microbial respiratory denitrification coupled with carbon oxidation. Alternatively, NO_3^- may be reduced by chemolithoautotrophic bacteria using sulfide as an electron donor. The aim of this study was to quantify the NO_3^- reduction process with sulfide oxidation under different NO_3^- input concentrations in river sediment.
Materials and methods Under NO_3^- input concentrations of 0.2 to 30 mM, flow-through reactors filled with river sediment from the Pearl River, China, were used to measure the processes of potential NO_3^- reduction and sulfate (SO_4^{2-}) production. Molecular biology analyses were conducted to study the microbial mechanisms involved.
Results and discussion Simultaneous NO_3^- removal and SO_4^{2-} production were observed with the different NO_3^- concentrations in the sediment samples collected at different depths. Potentially, NO_3^- removal reached 72 to 91 % and SO_4^{2-} production rates ranged from 0.196 to 0.903 mM h^{-1}. The potential NO_3^- removal rates were linearly correlated to the NO_3^- input concentrations. While the SO_4^{2-} production process became stable, the NO_3^- reduction process was still a first-order reaction within the range of NO_3^- input concentrations. With low NO_3^- input concentrations, the NO_3^- removal was mainly through the pathway of dissimilatory NO_3^- reduction to NH_4^+, while with higher NO_3^- concentrations the NO_3^- removal was through the denitrification pathway.
Conclusions While most of NO_3^- in the sediment was reduced by denitrifying heterotrophs, sulfide-driven NO_3^- reduction accounted for up to 26 % of the total NO_3^- removal under lower NO_3^- concentrations. The vertical distributions of NO_3^- reduction and SO_4^{2-} production processes were different because of the variable bacterial communities with depth.

Keywords Flow-through reactor · Nitrate reduction · Sediment · Sulfide oxidation

Responsible editor: Marcel van der Perk

X. Yang · S. Huang · Q. Wu (✉) · R. Zhang (✉)
School of Environmental Science and Engineering, Sun Yat-sen University, Guangdong Provincial Key Laboratory of Environmental Pollution Control and Remediation Technology, Guangzhou, Guangdong 510275, People's Republic of China
e-mail: eeswuqh@mail.sysu.edu.cn
e-mail: zhangrd@mail.sysu.edu.cn

1 Introduction

Anthropogenic activities have dramatically increased nitrogen (N) loading to aquatic ecosystems, particularly in the highly developing and densely populated regions (Galloway et al. 2004; Boyer et al. 2006). The N loading has resulted in considerable increase in nitrate (NO_3^-) concentrations in rivers, contributing to coastal eutrophication and hypoxia (Qiu et al. 2010). Nevertheless, most of the N loading to terrestrial soils and freshwater disappears before reaching coastal waters (Forshay and Stanley 2005; Seitzinger et al. 2006). These changes in N cycling lead to the question: what processes are involved in N removal from rivers?

Most attention has been devoted to study NO_3^- removal by respiratory denitrification with organic carbon as an electron donor, and dissimilatory NO_3^- reduction to ammonium (DNRA) by fermentative bacteria (Burgin and Hamilton 2007). Alternatively, autotrophic denitrifiers can use NO_3^- to oxidize sulfide and elemental S to SO_4^{2-} and their biogeochemical importance has been recognized (Jørgensen and Gallardo 1999; Shao et al. 2010). Nevertheless, most research activities have been focused on sulfide-driven autotrophic denitrifiers in marine sediments (Fossing et al.

1995; Sayama et al. 2005; Zhang et al. 2009). Several taxa, including the members of the genera *Thiobacillus*, *Thiocapsa*, and *Beggiatoa*, have been established with diverse metabolic characteristics (Brettar and Rheinheimer 1991; Jørgensen and Gallardo 1999; Kojima and Fukui 2003). More recently, the importance of sulfide-driven autotrophic denitrifiers in freshwater ecosystems has been investigated. For example, Kamp et al. (2006) enriched the *Beggiatoa* from a NO_3^--rich stream and observed its ability to oxidize sulfide with NO_3^-. Burgin and Hamilton (2008) studied the pathways of sulfide-driven NO_3^- reduction in freshwater bodies. Payne et al. (2009) revealed the coupling respond of N and S in wetlands.

There are two pathways for NO_3^- removal through sulfide oxidation: reducing NO_3^- to N_2 in the form of denitrification; and reducing NO_3^- to NH_4^+ in the form of DNRA (Burgin and Hamilton 2008). Environmental factors in river sediment, such as sediment depth, NO_3^- concentrations, and bacterial population and activities, should affect the NO_3^- removal process with S oxidation and the associated pathways. However, the potential and mechanisms of sulfide-driven NO_3^- reduction in river sediment are still poorly understood. Therefore, the objectives of this study were: (1) to investigate the potential rates of sulfide-driven NO_3^- reduction with different NO_3^- input concentrations in different depths of river sediment; and (2) to explore the dominate pathways of the sulfide-driven NO_3^- reduction process.

2 Materials and methods

2.1 Sample collection

Sediment samples were collected from a drain outlet (113° 17′1.66″E, 23°6′50.41″N) of the Pearl River in Guangzhou, China. The section Pearl River crossing Guangzhou City is close to the Pearl River Estuary, which links the highly developing urban area and the South China Sea, and represents an important ecosystem. In recent years, the Pearl River has been subjected to a high load of anthropogenic contaminants from wastewater runoff because of the increasing population and economic development in the Pearl River Delta (Jiang et al. 2009; Lu et al. 2009). The river is also affected by tides of the South China Sea.

On July 14th, 2010, two sediment cores were collected using a core sampler with a diameter of 7.0 cm and length of 50 cm. Water samples above the sediment–water interface, and the top 30 cm of the sediment cores were retained for the following experiments: (1) one of the sediment cores was used for flow-through reactor (FTR) experiments (described below); and (2) the other core was used to analyze chemical and microbial conditions of the sediment before the FTR experiments.

2.2 Flow-through reactor experiment

Six FTRs in this study were constructed following Pallud et al. (2007). The inner diameter of the reactor cell was the same as that of the sediment core (7.0 cm). A buffer room and a sintered disk were included to homogenize the influent. The 30 cm sediment core was cut into slices at depths of 0–2, 5–7, 10–12, 15–17, 20–22 and 25–27 cm. Each sediment slice was put into the polyvinyl chloride cell of the FTR with nitrocellulose filter (0.22 μm pore size) on each side.

The FTR experiments were conducted in an incubator, in which the temperature was set at 28 °C based on the temperatures of bottom water in the river (range from 12 to 28 °C). The influent of FTR was controlled at a constant flow rate (15 $cm^3\ h^{-1}$) using a peristaltic pump. Input solutions included five NO_3^- concentrations (0.2, 1, 5, 15 and 30 mM) and one Br^- solution (1 mM). The NO_3^- input concentrations were selected based on the literature (e.g., Laverman et al. 2007; Pallud et al. 2007). To ensure an anaerobic condition in the cell, each reactor was wrapped with airproof material and the input solution was vigorously purged with argon gas before entering the cell. For each input solution, the experiment was carried out until reaching a steady-state outflow concentration (about 20 h). The Br^- breakthrough curves were used to obtain the transport parameters (Pallud et al. 2007).

The steady-state rate of NO_3^- reduction or SO_4^{2-} production was calculated as follows:

$$R = \frac{(C_i - C_o)Q}{V} \quad (1)$$

where: C_i is the input concentration; C_o is the steady-state concentration in the outflow; Q is the volumetric flow rate; and V is the volume of the sediment slice in the reactor.

2.3 Analysis of environmental parameters

Water content of the sediment samples was measured using the gravimetric method. Concentrations of Br^-, NO_2^-, NO_3^- and SO_4^{2-} of the water samples, interstitial water samples from the sediment sub-samples, and the outflow samples of the FTR experiments were measured using ion chromatography (Metrohm 882, Metrohm AG, Herisau, Switzerland), and NH_4^+ using spectrophotometric detection with Nessleri's reagent. Total organic carbon content (TOC) was determined with the potassium dichromate dilution heat colorimetric method and the total nitrogen (TN) content was determined using a Foss Kjeltec 2300 Analyzer Unit (Foss Tecator AB, Höganäs, Sweden). Analyses of acid-volatile sulfur (AVS) concentrations in the sediment were based on the cold-acid purge-and-trap method (Chen et al. 2006).

2.4 Molecular biology analysis

2.4.1 DNA extraction and PCR amplification

Total DNA was extracted from each sediment slice with Fast DNA spin kit (Bio 101, Qbiogene Inc., CA, USA) following manufacturer's instruction manual. The following primer sets were used for PCR amplification of the genes encoding 16S rRNA: the forward primer 27F (5′-AGAGTTT GATCMTGGCTCAG-3′) labeled at the 5′ end with the dye carboxyfluorescein (FAM; synthesized within the primer by Genolab Co., Ltd., China.) and the reverse primer 1492R (5′-GGTTACCTTGTTACGACTT-3′). The PCR mixture contained 50 ng of extracted DNA, 2 μl of 5 mM concentrations of each primer, 3.2 μl of 2.5 mM concentrations of dNTP, 0.4 μl of 5 U/μl TaKaRa Taq DNA polymerase (TaKaRa Bio Inc., Shiga, Japan), and 5 μl of 10× PCR buffer for TaKaRa Taq, then replenish with ddH_2O to 50 μl. The PCR amplifications were performed in a total volume of 50 μl in 0.2 ml reaction tubes using the PCR reactor (T-gradient, Biometra, USA) with the following procedure, 94 °C for 5 min and then 30 cycles each consisting of 30 s at 94 °C, 30 s at 55 °C; and 45 s at 72 °C; and finally 10 min at 72 °C to complete the primer extension. The presence of PCR products was shown using 1 % agarose gel electrophoresis.

2.4.2 Terminal-restriction fragment length polymorphism analysis

After the processes of purification and concentration of the PCR products with a Wizard SV gel and a PCR clean-up system (AxyPrep PCR clean kit, China), 5 μl of the amplicons were digested with 10 U of the restriction enzyme *Hae*III, *Hha*I, and *Msp*I (TaKaRa, Japan), respectively, in the manufacturer's recommended reaction buffers for 4 h at 37 °C. Enzymes were subsequently inactivated by incubation at 65 °C for 20 min. Cleaved PCR products were purified by ethanol precipitation and dissolved in 20 μl of sterile ddH_2O. Ten μl of the purified products together with 0.5 μl of internal standard (ROX-500) were denatured at 95 °C for 2 min, cooled on ice, and subject to electrophoresis on a ABI 3730XL DNA analyzer (Applied Biosystems, USA). After electrophoresis, the size of the fluorescently labeled terminal-restriction fragments (T-RFs) was determined by comparing with the size standard using the software GeneMarker 1.97. To avoid detecting primers and uncertainties in size determination, terminal-restriction fragment lengths smaller than 50 bp were excluded. The percentage of detected T-RF was calculated from the peak height to the total peak height (>1 %). T-RFs were identified by the T-RFLP analysis package built by the Center for Limnology, University of Wisconsin–Madison, USA (https://secure.limnology.wisc.edu/trflp), then the taxonomy information was searched from the U.S. National Center for Biotechnology Information (http://www.ncbi.nlm.nih.gov).

2.4.3 Real-time PCR analysis

The primers selected for amplification of the different genes encoding *narG*, *nirS*, *nirK*, *nosZ* and *nrfA* are narG328f–narG497r (Reyna et al. 2010), nirS3f–nirS5r (Braker et al. 1998), nirK2f–nirK3r (Thräback et al. 2004), nos1527f–nos1773r (Scala and Kerkhof 1998), and nrfA2F–nrfA2R (Smith et al. 2007). Each assay contained a standard using a serial dilution of known copies of PCR fragments of the respective functional genes, independent triplicate sediment DNA templates for each sediment slice, and triplicate no template controls. Experimental Q-PCR triplicates for each DNA sample were then averaged to obtain a single gene copy number. Real-time PCRs were carried out in LightCycler480 with Sequence Detection Software v1.4 (Applied Biosystems, USA). Each PCR mixture (10 μl) was composed of 5 μl of SYBR Premix Ex TaqTM II (2×), 0.4 μl 10 nM of each forward and reverse primers, 0.2 μl ROX Reference Dye II (50×)×3, 3.2 μl ddH_2O and 2.0 μl of template DNA (TaKaRa Biotechnology, Japan). PCR amplification and detection were performed in LightCycler480 Multiwell (384-well) reaction plates with optical cap (Applied Biosystems, USA). The PCR procedure was as follows, 30 s at 94 °C, 40 cycles of 5 s at 94 °C; 30 s at the specific annealing temperature (61, 57, 57, 57, and 60 °C for *narG*, *nirS*, *nirK*, *nosZ*, and *nrfA*, respectively); and 30 s at 70 °C. A melting curve analysis for SYBR Green assay was conducted after the amplification to distinguish the targeted from the non-targeted PCR product.

3 Results

3.1 Physical and chemical characteristics of the sediment core

Physical and chemical properties of the sediment core are listed in Table 1, including water content, porosities, concentrations of NO_3^-, NH_4^+, TN, TOC and AVS of the sediment, and concentrations of NO_3^- and NH_4^+ in the interstitial water. The water contents and porosities decreased from 67 % to 29 % and from 82 % to 54 %, respectively, with increasing core depths. The NO_3^- concentrations in the sediment and interstitial water reached the maximum values (0.056 mmol kg^{-1} and 0.0802 mM, respectively) at a depth of 10-12 cm, then decreased with the depth. The NH_4^+ concentrations were much larger than the NO_3^- concentrations and the maximum NH_4^+ values in the sediment and interstitial water (39.0 mmol kg^{-1} and 5.48 mM,

Table 1 Physical and chemical characteristics of the sediment core

Depth	Water content	Porosity	Sediment					Interstitial water	
(cm)	%	%	NO_3^- (mmol kg^{-1})	NH_4^+ (mmol kg^{-1})	TN (g kg^{-1})	TOC (g kg^{-1})	AVS (mmol kg^{-1})	NO_3^- (mM)	NH_4^+ (mM)
0–2	67.6	81.8	0.038	14.1	1.11	15.2	12.0	0.0310	1.069
5–7	60.0	77.9	0.038	16.2	1.71	36.2	26.9	0.0273	1.547
10–12	54.0	74.2	0.056	39.0	2.80	57.1	25.0	0.0802	5.484
15–17	40.7	56.8	0.054	24.1	1.45	27.4	33.7	0.0255	1.211
20–22	36.9	63.2	0.039	22.3	1.40	20.3	27.1	0.0283	2.671
25–27	28.6	53.6	0.037	29.5	1.44	18.9	27.6	0.0291	2.109

respectively) also occurred at a depth of 10-12 cm. The TOC and TN values were highly correlated with a coefficient of determination (R^2) of 0.934 ($p<0.05$) and their peak values were also at 10–12 cm depth. The AVS concentration in the surface layer (12.0 mmol kg^{-1}) was significantly lower than in deeper layers (see Table 1). The highest AVS (33.7 mmol kg^{-1}) was in the 15–17 cm layer, while the AVS values in other layers ranged from 25.0 to 27.6 mmol kg^{-1}.

3.2 Nitrate removal in the flow-through reactor

Nitrate removal was observed in the FTR experiments with the different NO_3^- input concentrations. The NO_3^- removal in the sediment samples at the different depths ranged from 72 to 91 %. Higher NO_3^- removal percentages were observed with the lower input concentrations (0.2 and 1 mM). With the increase of input concentrations, the removal percentages of NO_3^- decreased from 85 to 75 %. The variability of the NO_3^- removal percentages among the different sediment depths was small, as indicated by the small range of the quartile intervals (0.68 to 1.58 %).

The potential NO_3^- removal rates in the FTRs were linearly related to the NO_3^- concentrations in the reactor with high R^2 values, ranging from 0.9974 to 0.9996. For all the sediment samples at the different depths, the linear relationships were almost identical with slopes ranging from 0.223 to 0.230 and intercepts ranging from 0.0365 to 0.0540. All the linear relationships can be represented by the following relationship:

$$R_p = 0.045 + 0.226C_r \quad (2)$$

where: R_p is the potential NO_3^- removal rates; and C_r is the NO_3^- concentration in the reactor, calculated by the average of the input and output NO_3^- concentrations. The equation indicated that, in this range of input concentrations (0.2–30 mM), the potential NO_3^- removal rates in all layers of the sediment were of a first-order reaction with the maximum removal rate of 3.877 mM h^{-1}.

3.3 Sulfate production in the flow-through reactor

When the NO_3^- input concentration increased from 0.2 to 30 mM, SO_4^{2-} production values increased correspondingly (Table 2). The SO_4^{2-} production rates in all sediment depths also increased significantly with the NO_3^- removal (Fig. 1). The SO_4^{2-} production rates were more variable among the different depths compared to the NO_3^- removal rates. In particular, when the NO_3^- input concentrations ≥5 mM, the differences of SO_4^{2-} production rates among the depths became more obvious. At a depth of 20–22 cm, the SO_4^{2-} production rates increased significantly with the NO_3^- input concentrations, while at a depth of 10–12 cm the SO_4^{2-} production rates did not respond to the NO_3^- inputs as strongly as at other depths. The SO_4^{2-} production rates decreased from the surface to 10–12 cm then increased at deeper depths.

Table 2 Sulfate production under different nitrate input concentrations ($n=3$)

Concentration of NO_3^- input (mM)	Concentration of SO_4^{2-} production (mM)					
	0–2 cm	5–7 cm	10–12 cm	15–17 cm	20–22 cm	25–27 cm
0.2	0.031±0.000	0.030±0.004	0.029±0.003	0.027±0.003	0.057±0.002	0.054±0.006
1	0.063±0.003	0.081±0.003	0.047±0.005	0.070±0.002	0.110±0.006	0.057±0.000
5	0.132±0.007	0.100±0.274	0.077±0.004	0.123±0.029	0.282±0.023	0.148±0.009
15	0.303±0.006	0.238±0.019	0.141±0.006	0.165±0.016	0.480±0.013	0.189±0.009
30	0.439±0.018	0.388±0.061	0.166±0.020	0.443±0.023	0.578±0.006	0.257±0.035

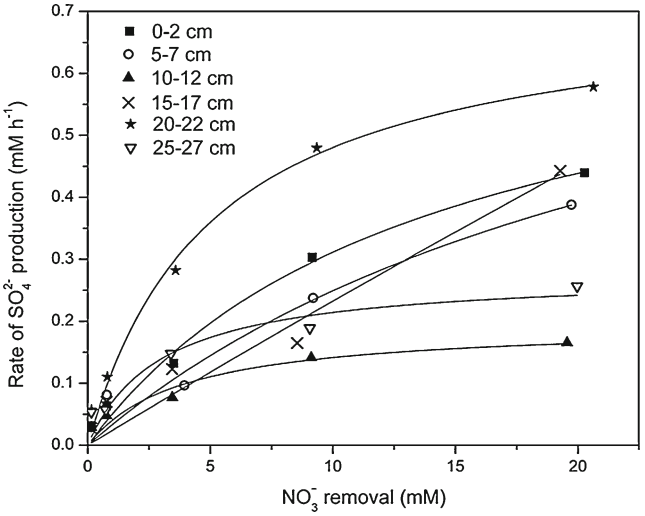

Fig. 1 Sulfate production rates vs. nitrate removal (with best-fit curves using the Michaelis–Menten function) at different sediment depths for a core collected from the Pearl River, China

3.4 Ammonium production in the flow-through reactor

In contrast to the SO_4^{2-} production, NH_4^+ production did not increase with the increased NO_3^- concentrations (Fig. 2). On average, the highest NH_4^+ production was about 0.342 mM and was reached at the low NO_3^- input concentration (0.2 mM). Subsequently, NH_4^+ production decreased with increased NO_3^- input concentrations and became stable (0.198 to 0.217 mM) with the higher NO_3^- input concentrations.

3.5 The abundances of denitrification functional genes

The vertical distributions of denitrification functional genes (*narG*, *nirS*, *nirK*, and *nosZ*) before and after the FTR experiments were markedly different (Figs. 3a–d), while the *nrfA* gene could not be quantified due to its poor amplification efficiency. The *narG* gene encoded to NO_3^- reductase significantly increased from 1.85×10^3 to 5.72×10^3 g^{-1} sediment on average after the FTR experiments, especially for the top three layers. The *nirS* gene encoded to nitrite (NO_2^-) reductase (a cytochrome cd1) increased after the FTR experiments within the top and bottom layers. In contrast, the *nirK* gene encoded to another type of NO_2^- reductase (a Cu-containing enzyme) reduced by one to two orders of the magnitude, with very small variability with depth. Similarly, the *nosZ* gene encoded to nitrous oxide reductase declined dramatically from 1.21×10^3 to 0.39×10^3 g^{-1} sediment.

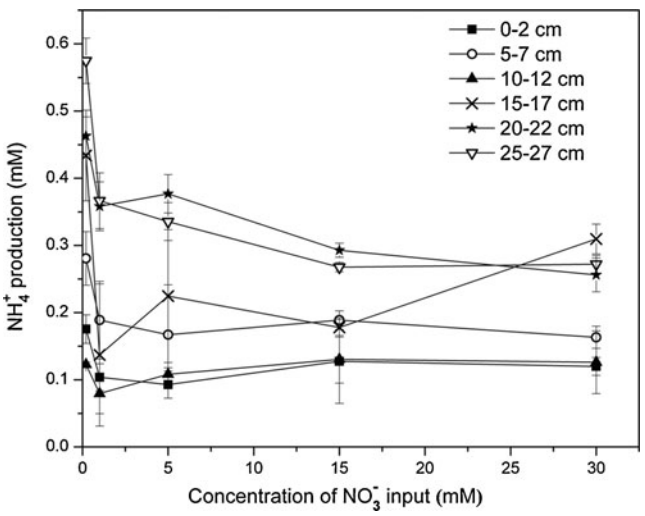

Fig. 2 Ammonium production vs. different nitrate input concentrations at different sediment depths. Values are expressed as mean ±standard deviation (n=3)

3.6 Analysis of terminal-restriction fragment length polymorphism

The microbial populations were characterized by the analysis of T-RFLP profiles using 16S rRNA. Its relative abundance was based on the T-RFLP profiles digested by restriction of the enzyme *Hae*III. To identify the probable microbial species, the information on terminal-restriction fragment digested by *Hha*I and *Msp*I was used conjointly with that for *Hae*III. After the FTR experiment, at least one prominent peak (the length of the predominant T-RFs) became more prominent. Overall, two peaks, accounting for the most proportion of integral areas, appeared in five reactors except the one at 20–22 cm depth. Peak 329 bp in T-RFLP fingerprints was observed in the reactors with sediment samples at 0–2, 5–7, and 25–27 cm depth, accounting for 34, 12, and 1.4 % of their total integral areas, respectively. Peak 334 bp was observed in the reactors at 10-12 and 15-17 cm depth, accounting for 67 % and 72 % of total integral areas, respectively. Peaks of 329 and 334 bp matched well *Lactobacillus*. Highly similar gene fingerprints were observed after the FTR experiment, suggesting that the same population of bacteria had been colonized in the different sediment layers by the stimulation of NO_3^-. In contrast to the ubiquitous peaks, the main T-RFs were observed only in some layers. For example, *Thiobacillus* and *Thiocapsa* matched with peaks of 78 and 243 bp in the layers at 10–12, 15–17, and 25–27 cm depth, while *Beggiatoa* (matched with peak 189 bp) appeared at 0–2 and 5–7 cm depth after the FTR experiments. A significant proportion of the different T-RFLP peaks were observed only at 20–22 cm depth. *Spirochaeta halophila* (M88722, matched with peak 206 bp), which was closely related to green sulfur bacteria (Woese et al. 1990), accounted for 8.9 % of total integral area. This was a high percentage compared with the sulfide oxidizing bacterium genus above.

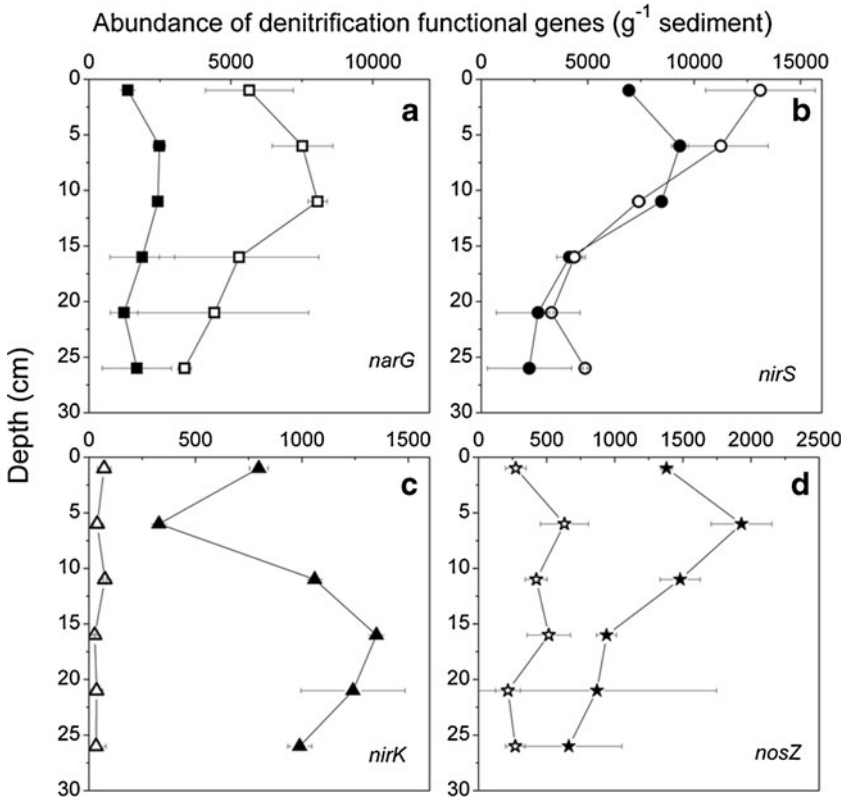

Fig. 3 Vertical distributions of **a** *narG*, **b** *nirS*, **c** *nirK*, and **d** *nosZ* before (*solid symbol*) and after (*open symbol*) the flow-through reactor experiments. Values are expressed as mean ±standard deviation (n=3)

4 Discussion

4.1 Vertical distributions of C, N, and S in the sediment core

The vertical distributions of nutrients should influence bacterial communities at different sediment depths (Fan et al. 2006; Huang et al. 2011). Long-term domestic wastewater pollution has resulted in organic matter accumulation in the sediment, which provides adequate nutrition for microbial growth. Thus, the high activities of microbes should influence the distributions and transformation of the inorganic N. Generally, NO_3^- and TOC decrease with sediment depth, and the denitrification of deeper sediments can be neglected due to substrate limitation (Tiquia et al. 2006). However, the vertical distribution of inorganic N in our sediment had a peak value at 10–12 cm depth instead of at the surface. The NO_3^- concentrations of the deep layers were similar to those of the top layers. Therefore, N cycling might also be active in the deeper sediment layers. Nitrite was below detection in most samples. Nevertheless, the NH_4^+ concentrations were higher than those in other sediments (Magalhães et al. 2005; Fan et al. 2006; Strous et al. 2006). The high NH_4^+ concentrations might result from active mineralization of organic N (Farías et al. 2004), which is typical for an urban river. In the sediment, the high concentrations of NH_4^+, which is the substrate of nitrification and product of dissimilation, may influence the rate and pathway of microbial processes (Ma and Aelion 2005). The AVS concentrations in our sediment were comparable with those in other river sediments collected in the Pearl River Delta, China (Sheng et al. 2011) and were higher than those in the Pearl River Estuary (Chen et al. 2006).

4.2 Nitrate removal with sulfate production

Nitrate removal is generally considered to be a beneficial process in aquatic ecosystems (Brunet and Garcia-Gil 1996). Nitrate removal also enhances the process of sulfide oxidation. The NO_3^- input in the FTR experiments showed high percentages of NO_3^- removal and high NO_3^- potential removal rates. The potential NO_3^- removal rates reported here were higher than those in other fresh water sediments and in marine sediments (Hordijk et al. 1987; Laverman et al. 2006, 2007; Pallud et al. 2007). In the FTR experiments, the NO_3^- removal rates remained as a first-order reaction when the NO_3^- input concentrations increased 150 times (from 0.2 to 30 mM). The high initial concentration of TOC at the study site supported labile products from organic matter decomposition, which was beneficial to the NO_3^- removal process. At our site in the subtropical zone, the high water temperature promoted the NO_3^- removal process (Piña-Ochoa and Álvarez-Cobelas 2006; Silvennoinen et al. 2008; Li et al. 2010). Based on the literature, the wide range of the NO_3^- input concentrations was selected to study the potential NO_3^- removal rates in the sediment. In addition, NO_3^- concentrations of overlying water in certain water bodies, such as in Pearl River (Dai et al. 2006) and Marne

River, France (Laverman et al. 2010), are within the range of the NO_3^- input concentrations in this study. Therefore, the results here should be useful to estimate the actual NO_3^- removal rates.

Sulfate production coincident with NO_3^- removal was observed at all depths and all NO_3^- input concentrations in the FTR experiments (see Table 2), which was evidence of the sulfide-driven NO_3^- reduction process. The SO_4^{2-} production was highly related to the NO_3^- input, indicating that the biologically mediated process, instead of the O_2-driven S oxidation process, promoted the sulfide-driven NO_3^- reduction process. In addition, the experiments were conducted under an anaerobic condition. In our experiments, the NO_3^- addition stimulated NO_3^- reducers and acted as an electron acceptor in anaerobic metabolism for sulfide oxidizers, ultimately enhancing production of SO_4^{2-}. The sulfide-driven NO_3^- reduction process was consistent with that reported in the literature (Burgin and Hamilton 2008; Payne et al. 2009). The common electron acceptors, in order from the highest to lowest efficiency of energy, are O_2, NO_3^-, Fe^{3+} and SO_4^{2-}. Microbes utilizing electron acceptors with a higher efficiency should be more competitive (Burgin and Hamilton 2007). In an anaerobic condition, NO_3^- has a higher energy efficiency than SO_4^{2-}. Denitrifiers (i.e., sulfur oxidizers) can easily use NO_3^- as an electron acceptor, oxidizing reduced S to SO_4^{2-}. At our study site, the load of reduced sulfur (such as AVS) from the protein mineralization in domestic wastewater might be the main reason for SO_4^{2-} production corresponding to NO_3^- reduction.

We investigated the SO_4^{2-} production under different NO_3^- input concentrations. As illustrated in Fig. 1, the SO_4^{2-} production rates did not increase with the NO_3^- removal linearly. The results were explained as follows. Because of the high NO_3^- removal rates, the electron acceptors (NO_3^-) were always rich in the reactions. Therefore, NO_3^- was not a limiting factor for the processes of reducing NO_3^- to N_2 in the form of denitrification and for reducing NO_3^- to NH_4^+ in the form of DNRA. Although some forms of reduced sulfur are not available for microbial NO_3^- reduction (Haaijer et al. 2007), the amount of reactive reduced sulfur (AVS) in this study was sufficient for the sulfide-driven NO_3^- reduction process. The process was mainly controlled by the electrons transferred in the reaction of S^{2-} oxidizing to SO_4^{2-} by relative bacteria. The SO_4^{2-} production rates driven by NO_3^- removal could be characterized by the Michaelis–Menten function as follows (Laverman et al. 2010):

$$R_s = R_{\max}\frac{C}{K_m + C} \tag{3}$$

where: R_s is the SO_4^{2-} production rate; C is the concentration of NO_3^- removal in the reactor; $R_{\max}$ is the maximum reaction rate; and K_m is the half-saturation concentration. As shown in Fig. 1, the data were fitted well by Eq. (3), with an R^2 of 0.900 to 0.988. From the fitting, we also obtained the maximum SO_4^{2-} production rates ($R_{\max}$) ranging from 0.196 to 0.903 mM h^{-1}.

The molar ratio of SO_4^{2-} production to NO_3^- removal (SP/NR) indicates the relative importance of SO_4^{2-} production in NO_3^- removal (Burgin and Hamilton 2008). In this study, the ratio of SP/NR decreased from 26 to 1.9 % with the increase of NO_3^- input concentrations. The results suggest that the sulfide-driven NO_3^- reduction process could not be neglected because it accounted for up to 26 % of the total NO_3^- removal under the low NO_3^- condition (0.2 mM).

4.3 The pathways of nitrate reduction with sulfide oxidation

In the FTR experiments, the NO_3^- removal reached 72 to 91 % and NO_2^- was hardly detected from the FTR output. The increase of *nirS* genes also indicated active NO_2^- reduction. There were three possible pathways of NO_3^- and NO_2^- reduction in this process (Burgin and Hamilton 2007), i.e.: denitrification ($NO_3^- \rightarrow NO_2^- \rightarrow NO \rightarrow N_2O \rightarrow N_2$); DNRA ($NO_3^- \rightarrow NO_2^- \rightarrow NH_4^+$); and anaerobic ammonia oxidation (ANAMMOX) ($NO_2^- + NH_4^+ \rightarrow N_2H_4 \rightarrow N_2$). ANAMMOX is restricted to low NO_3^- concentrations and comparative low C/N ratios (Burgin and Hamilton 2007). Its contribution to N_2 release only accounts for 8 % in estuary sediment and 2 % in eutrophic marine sediment (Thamdrup and Dalsgaard 2002; Trimmer et al. 2003). With the high NO_3^- concentrations in the FTR experiments, ANAMMOX should not be the main process.

Compared to denitrification, DNRA is a relatively understudied pathway of microbial metabolism (Burgin and Hamilton 2007). The DNRA is considered to be promoted by fermentation (Tiedje 1988). The pathway is often coupled with sulfur cycling and iron transfer (Korom 1992; An and Gardner 2002; Weber et al. 2006), though it is still unknown whether the two processes are mutually exclusive (Burgin and Hamilton 2007). Organic-rich and NO_3^--limited conditions favor the DNRA pathway (Megonigal et al. 2004; Laverman et al. 2006), while NO_3^--sufficient conditions with a suitable C/N ratio favor denitrification (Silver et al. 2001). To study the DNRA results, we measured NH_4^+ concentrations from the water output. Interestingly, the NH_4^+ production decreased with increased NO_3^- input concentrations (see Fig. 2), which was different from the general recognition that NO_3^- addition stimulates the DNRA aggrandizement (An and Gardner 2002). The ratio of NH_4^+ production to NO_3^- removal in our study (1.04 to 6.07 % over 1 mM NO_3^- input) showed that NH_4^+ production only accounted for a small fraction of the NO_3^- removal. The explanation of the result was related to environmental conditions (Burgin and Hamilton 2007). The low C/N resulted from the high labile carbon concentration (see Table 1) with

the high NO_3^- inputs leading to high efficiency of respiratory denitrification. As shown in Fig. 4, the ratio of NH_4^+ production rates to NO_3^- reduction rates (APR/NRR) described the theoretical threshold lines for the different processes (Laverman et al. 2006). With the low concentration (0.2 mM) of NO_3^- input, APR/NRR values at all depths (except for 10–12 cm) were larger than 1.15, indicating that the DNRA was the main pathway of NO_3^- removal. However, with an increase of the NO_3^- input concentrations, the processes tended to shift to denitrification and incomplete denitrification. Laverman et al. (2006) assumed that the end-product of incomplete denitrification was NO_2^-. However, in our study, the absence of NO_2^- in the FTR output and the increase of *nirS* gene after the FTR culture suggested that NO_2^- was probably transformed to NO, then to N_2O.

Sulfide reduction may interfere with both denitrification (Fossing et al. 1995) and DNRA (Sayama et al. 2005). A high H_2S concentration can inhibit denitrification and lead NO_3^- to transfer to NH_4^+ (An and Gardner 2002; Mazéas et al. 2008). A low H_2S concentration should stimulate NO_3^- removal and inhibit denitrification at the same time, which resulted in N_2O accumulation (Senga et al. 2006; Aelion and Warttinger 2009; Beristain-Cardoso et al. 2009). On the other hand, elemental S and metal-bound sulfides often present in fresh sediments should spur on S oxidizers to participate in denitrification (Burgin and Hamilton 2007). In this study, the H_2S might be quickly consumed in the early stage of the FTR experiment. The ratio values of SO_4^{2-} and NH_4^+ productions ranged from 13.7 to 197 % (calculated from the SP/AR) with the increase of NO_3^- input concentrations. Therefore, sulfide might stimulate the DNRA process with the low NO_3^- concentrations (0.2–1.0 mM) and be involved in the denitrification with the higher NO_3^- inputs (over 5.0 mM).

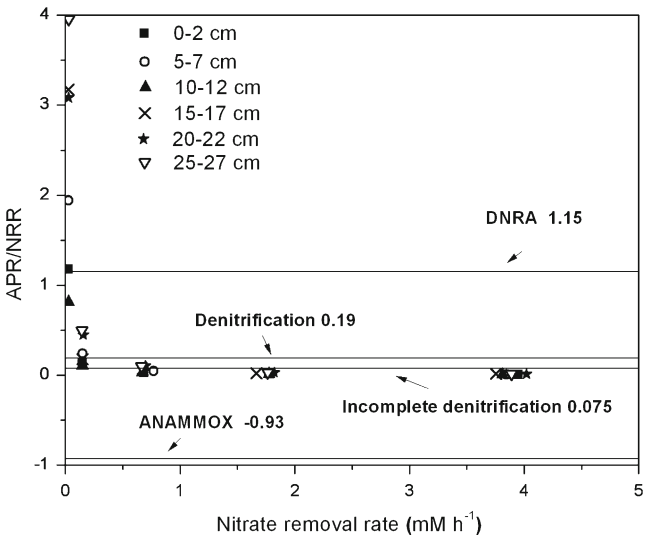

Fig. 4 Ratios of ammonium production rates vs. nitrate reduction rates (APR/NRR) as a function of nitrate removal rates in sediment samples at different depths

4.4 Vertical distributions of the sulfide-driven nitrate reduction

The NO_3^- removal capacity in each layer of the sediment was almost the same (Eq. 2), which was mainly attributable to the substrate concentrations and environment conditions, with sufficient NO_3^- and organic matter at all sediment depths. Adequate substrates enhanced NO_3^- reducers to gain a competitive advantage. Similar prominent peaks appeared in all the T-RFLP profiles after the FTR experiments. The peaks matched *Lactobacillus*, which is a NO_2^- reducer with products of N_2O and CO_2 (Dodds and Collins-Thompson 1985). The predominating population in the FTR kept the high rates of denitrification and mineralization. The *narG* genes amassed at depths of 5–7 cm and 10–12 cm before the FTR experiments and became uniform after the experiments, which was another line of evidence for the similar NO_3^- reduction rates in all sediment layers. However, with lower NO_3^- input concentrations, the NO_3^- reduction pathways were different in the different layers (see Fig. 4). The N and C aggregation layer (10–12 cm) resulted in denitrification process with 0.2 mM NO_3^- input.

In this study, the amount of AVS in each sediment slice was sufficient for the sulfide oxidation process. Therefore, the difference of SO_4^{2-} production among the depths might be caused by the diversity of sulfide oxidizers in the different layers. *Thiobacillus*, *Thiocapsa*, and *Beggiatoa* identified in this study belong to the autotrophic denitrifiers (Zopfi et al. 2001; Kamp et al. 2006; Shao et al. 2010). However, *Beggiatoa* only appeared in the upper layers after the FTR experiments, while *Thiobacillus* and *Thiocapsa* only appeared in the deep layers. The relatively high abundance of *S. halophila* at 20–22 cm depth after the FTR experiments might be the reason for the highest SO_4^{2-} production among the layers. More accurate characterization of the microbial community among the layers is currently under investigation.

5 Conclusions

Flow-through reactor experiments with river sediment samples from depths of 0 to 30 cm and influent NO_3^- concentrations of 0.2 to 30 mM were conducted to quantify the NO_3^- removal process with SO_4^{2-} production. Molecular biology analyses were carried out to study the microbial processes involved. With the different NO_3^- input concentrations and the different sediment samples, the NO_3^- removal reached 72 to 91 % and increased with SO_4^{2-} production. The potential SO_4^{2-} production rates ranged from 0.196 to 0.903 mM h^{-1}. With the NO_3^- input concentration of 0.2 mM, the main pathway of NO_3^- reduction in the FTR experiments was through DNRA, whereas with higher NO_3^- input concentrations the main pathway of

NO_3^- reduction was through denitrification. The results of NO_3^- removal at different depths were similar. Nevertheless, the results of SO_4^{2-} production along the depths were different because of the spatial variation of sulfide oxidation organisms. The results from this study should be useful to help understand the potential processes of N removal from rivers and their sediments.

Acknowledgments This work was partly supported by grants from the Chinese National Natural Science Foundation (Nos. 51039007 and 51179212) and the Fundamental Research Funds for the Central Universities.

References

Aelion CM, Warttinger U (2009) Low sulfide concentrations affect nitrate transformations in freshwater and saline coastal retention pond sediments. Soil Biol Biochem 41:735–741

An S, Gardner WS (2002) Dissimilatory nitrate reduction to ammonium (DNRA) as a nitrogen link versus denitrification as a sink in a shallow estuary (Laguna Madre/Baffin Bay, Texas). Mar Ecol Prog Ser 237:41–50

Beristain-Cardoso R, Texier A, Sierra-Álvarez R, Razo-Flores E, Field JA, Gomez J (2009) Effect of initial sulfide concentration on sulfide and phenol oxidation under denitrifying conditions. Chemosphere 74:200–205

Boyer EW, Howarth RW, Galloway JN, Dentener FJ, Green PA, Vörösmarty CJ (2006) Riverine nitrogen export from the continents to the coasts. Global Biogeochem Cycle 20:GB1S91

Braker G, Fesefeldt A, Witzel K (1998) Development of PCR primer systems for amplification of nitrite reductase genes (*nirK* and *nirS*) to detect denitrifying bacteria in environmental samples. Appl Environ Microb 64:3769–3775

Brettar I, Rheinheimer G (1991) Denitrification in the central Baltic: evidence for H_2S-oxidation as motor of denitrification at the oxic–anoxic interface. Mar Ecol Prog Ser 77:157–169

Brunet RC, Garcia-Gil LJ (1996) Sulfide-induced dissimilatory nitrate reduction to ammonia in anaerobic freshwater sediments. FEMS Microbiol Ecol 21:131–138

Burgin AJ, Hamilton SK (2007) Have we overemphasized the role of denitrification in aquatic ecosystems? A review of nitrate removal pathways. Front Ecol Environ 5:89–96

Burgin AJ, Hamilton SK (2008) NO_3-driven SO_4^{2-} production in freshwater ecosystems: Implications for N and S cycling. Ecosystems 11:908–922

Chen F, Yang Y, Zhang D, Zhang L (2006) Heavy metals associated with reduced sulfur in sediments from different deposition environments in the Pearl River estuary, China. Environ Geochem Health 28:265–272

Dai M, Wang L, Guo X, Zhai W, Li Q, He B, Kao S-J (2006) Nitrification and inorganic nitrogen distribution in a large perturbed river/estuarine system: the Pearl River Estuary, China. Biogeosciences 5:1227–1244

Dodds KL, Collins-Thompson DL (1985) Production of N_2O and CO_2 during the reduction of NO_2^- by *Lactobacillus lactis* TS4. Appl Environ Microb 50:1550–1552

Fan LF, Shieh WY, Wu WF, Chen CP (2006) Distribution of nitrogenous nutrients and denitrifiers strains in estuarine sediment profiles of the Tanshui River, northern Taiwan. Estuar Coast Shelf Sci 69:543–553

Farías L, Graco M, Ulloa O (2004) Temporal variability of nitrogen cycling in continental-shelf sediments of the upwelling ecosystem off central Chile. Deep-Sea Res Pt Ii 51:2491–2505

Forshay KJ, Stanley EH (2005) Rapid nitrate loss and denitrification in a temperate river floodplain. Biogeochemistry 75:43–64

Fossing H, Gallardo VA, Jørgensen BB et al (1995) Concentration and transport of nitrate by the mat-forming sulfur bacterium *Thioploca*. Nature 374:713–715

Galloway JN, Dentener FJ, Capone DG et al (2004) Nitrogen cycles: past, present, and future. Biogeochemistry 70:153–226

Haaijer SCM, Lamers LPM, Smolders AJP, Jetten MSM, Op den Camp HJM (2007) Iron sulfide and pyrite as potential electron donors for microbial nitrate reduction in freshwater wetlands. Geomicrobiol J 24:391–401

Hordijk CA, Snieder M, Van Engelen JJM, Cappenberg TE (1987) Estimation of bacterial nitrate reduction rates at in situ concentrations in freshwater sediments. Appl Environ Microbiol 53:217–223

Huang S, Chen C, Yang X, Wu Q, Zhang R (2011) Distribution of typical denitrifying functional genes and diversity of the *nirS*-encoding bacterial community related to environmental characteristics of river sediments. Biogeosciences 8:5251–5280

Jiang LJ, Zheng YP, Peng XT (2009) Vertical distribution and diversity of sulfate-reducing prokaryotes in the Pearl River estuarine sediments, Southern China. FEMS Microbiol Ecol 70:249–262

Jørgensen BB, Gallardo VA (1999) *Thioploca* spp.: filamentous sulfur bacteria with nitrate vacuoles. FEMS Microbiol Ecol 28:301–313

Kamp A, Stief P, Schulz-Vogt HN (2006) Anaerobic sulfide oxidation with nitrate by a freshwater *Beggiatoa* enrichment culture. Appl Environ Microb 72:4755–4760

Kojima H, Fukui M (2003) Phylogenetic analysis of *Beggiatoa* spp. from organic rich sediment of Tokyo Bay, Japan. Water Res 37:3216–3223

Korom SF (1992) Natural denitrification in the saturated zone: a review. Water Resour Res 28:1657–1668

Laverman AM, Van Cappellen P, van Rotterdam-Los D, Pallud C, Abell J (2006) Potential rates and pathways of microbial nitrate reduction in coastal sediments. FEMS Microbiol Ecol 58:179–192

Laverman AM, Canavan RW, Slomp CP, Van Cappellen P (2007) Potential nitrate removal in a coastal freshwater sediment (Haringvliet Lake, The Netherlands) and response to salinization. Water Res 41:3061–3068

Laverman AM, Garnier JA, Mounier EM, Roose-Amsaleg CL (2010) Nitrous oxide production kinetics during nitrate reduction in river sediment. Water Res 44:1753–1764

Li F, Yang R, Ti C, Lang M, Kimura SD, Yan X (2010) Denitrification characteristics of pond sediments in a Chinese agricultural watershed. Soil Sci Plant Nutr 56:66–71

Lu FH, Ni HG, Liu F, Zeng EY (2009) Occurrence of nutrients in riverine runoff of the Pearl River Delta, South China. J Hydrol 376:107–115

Ma HB, Aelion CM (2005) Ammonium production during microbial nitrate removal in soil microcosms from a developing marsh estuary. Soil Biol Biochem 37:1869–1878

Magalhães CM, Joye SB, Moreira RM, Wiebe WJ, Bordalo AA (2005) Effect of salinity and inorganic nitrogen concentration on nitrification and denitrification rates in intertidal sediments and rocky biofilms of the Douro River estuary, Portugal. Water Res 39:1783–1794

Mazéas L, Vigneron V, Le-Menach K, Budzinski H, Audic JM, Bernet N, Bouchez T (2008) Elucidation of nitrate reduction pathways in anaerobic bioreactors using a stable isotope approach. Rapid Commun Mass Spectrom 22:1746–1750

Megonigal JP, Hines ME, Visscher PT (2004) Anaerobic metabolism: linkages to trace gases and aerobic processes. In: Schlesinger WH (ed) Biogeochemistry. Elsevier-Pergamon, Oxford, pp 317–424

Pallud C, Meile C, Laverman AM, Abell J, Van Cappellen P (2007) The use of flow-through sediment reactors in biogeochemical kinetics: methodology and examples of applications. Mar Chem 106:256–271

Payne EK, Burgin AJ, Hamilton SK (2009) Sediment nitrate manipulation using porewater equilibrators reveals potential for N and S coupling in freshwaters. Aquat Microb Ecol 54:233–241

Piña-Ochoa E, Álvarez-Cobelas M (2006) Denitrification in aquatic environments: a cross-system analysis. Biogeochemistry 81:111–130

Qiu D, Huang L, Zhang J, Lin S (2010) Phytoplankton dynamics in and near the highly eutrophic Pearl River Estuary, South China Sea. Cont Shelf Res 30:177–186

Reyna L, Wunderlin DA, Genti-Raimondi S (2010) Identification and quantification of a novel nitrate-reducing community in sediments of Suquía River basin along a nitrate gradient. Environ Pollut 158:1608–1614

Sayama M, Risgaard-Petersen N, Nielsen LP, Fossing H, Christensen PB (2005) Impact of bacterial NO_3^- transport on sediment biogeochemistry. Appl Environ Microb 71:7575–7577

Scala DJ, Kerkhof LJ (1998) Nitrous oxide reductase (*nosZ*) gene-specific PCR primers for detection of denitrifiers and three *nosZ* genes from marine sediments. FEMS Microbiol Lett 162:61–68

Seitzinger S, Harrison JA, Bohlke JK, Bouwman AF, Lowrance R, Peterson B, Tobias C, Van Drecht G (2006) Denitrification across landscapes and waterscapes: a synthesis. Ecol Appl 16:2064–2090

Senga Y, Mochida K, Fukumori R, Okamoto N, Seike Y (2006) N_2O accumulation in estuarine and coastal sediments: the influence of H_2S on dissimilatory nitrate reduction. Estuar Coast Shelf Sci 67:231–238

Shao M, Zhang T, Fang HH (2010) Sulfur-driven autotrophic denitrification: diversity, biochemistry, and engineering applications. Appl Microbiol Biotechnol 88:1027–1042

Sheng Y, Fu G, Chen F, Chen J (2011) Geochemical characteristics of inorganic sulfur in Shijing River, South China. J Environ Monit 13:807–812

Silvennoinen H, Liikanen A, Torssonen J, Stange CF, Martikainen PJ (2008) Denitrification and N_2O effluxes in the Bothnian Bay (northern Baltic Sea) river sediments as affected by temperature under different oxygen concentrations. Biogeochemistry 88:63–72

Silver WL, Herman DJ, Firestone MK (2001) Dissimilatory nitrate reduction to ammonium in upland tropical forest soils. Ecology 82:2410–2416

Smith CJ, Nedwell DB, Dong LF, Osborn AM (2007) Diversity and abundance of nitrate reductase genes (*narG* and *napA*), nitrite reductase genes (*nirS* and *nrfA*), and their transcripts in estuarine sediments. Appl Environ Microb 73:3612–3622

Strous M, Pelletier E, Mangenot S et al (2006) Deciphering the evolution and metabolism of an anammox bacterium from a community genome. Nature 440:790–794

Thamdrup B, Dalsgaard T (2002) Production of N_2 through anaerobic ammonium oxidation coupled to nitrate reduction in marine sediments. Appl Environ Microb 68:1312–1318

Thräback IN, Enwall K, Jarvis A, Hallin S (2004) Reassessing PCR primers targeting *nirS*, *nirK* and *nosZ* genes for community surveys of denitrifying bacteria with DGGE. FEMS Microbiol Ecol 49:401–417

Tiedje JM (1988) Ecology of denitrification and dissimilatory nitrate reduction to ammonium. In: Zehnder AJB (ed) Environmental microbiology of anaerobes. Wiley, New York, pp 179–244

Tiquia SM, Masson SA, Devol A (2006) Vertical distribution of nitrite reductase genes (*nirS*) in continental margin sediments of the Gulf of Mexico. FEMS Microbiol Ecol 58:464–475

Trimmer M, Nicholls JC, Deflandre B (2003) Anaerobic ammonium oxidation measured in sediments along the Thames estuary, United Kingdom. Appl Environ Microb 69:6447–6454

Weber KA, Urrutia MM, Churchill PF, Kukkadapu RK, Roden EE (2006) Anaerobic redox cycling of iron by freshwater sediment microorganisms. Environ Microbiol 8:100–113

Woese CR, Mandelco L, Yang D, Gherna R, Madigan MT (1990) The case for relationship of the flavobacteria and their relatives to the green sulfur bacteria. Syst Appl Microbiol 13:258–262

Zhang T, Zhang M, Shao MF, Fang HHP (2009) Autotrophic denitrification in nitrate-induced marine sediment remediation and Sulfurimonas denitrificans-like bacteria. Chemosphere 76:677–682

Zopfi J, Kjaer T, Nielsen LP, Jørgensen BB (2001) Ecology of *Thioploca* spp.: nitrate and sulfur storage in relation to chemical microgradients and influence of *Thioploca* spp. on the sedimentary nitrogen cycle. Appl Environ Microb 67:5530–5537